POAC'11
Montréal, Canada
POAC11-007

Proceedings of the 21st International Conference on
Port and Ocean Engineering under Arctic Conditions
July 10-14, 2011
Montréal, Canada

EXPERIEMENTS ON THE RELATION BETWEEN FREEZE-BOND AND ICE RUBBLE STRENGTH, PART I: SHEAR BOX EXPERIMENTS

[1]Nicolas Serré, [2]Ada H. V. Repetto-Llamazares, Knut V. Høyland[3]

[1]NTNU, Department of Civil and Transport Engineering,
Høgskoleringen 7a, 7034 Trondheim, Norway.

[2]Barlindhaug Consult AS,
Sjølundveien 2, Tromsø, Norway.

ABSTRACT

The freeze-bond effects on the resistance of floating ice ridges and their deformation process is investigated. The results from 14 shear box tests are presented in this paper (part I) together with a preliminary analyse. Part II gives results from individual freeze-bond tests and a comparison between experimental and numerical shear box tests.

The rubble was composed of 60 x 40 x 22 mm saline ice blocks. Freeze-bonds with three different strength levels were created in the rubble by submerging it during 0 min, 10 min and 20 hours. The rubble was tested in a 600 x 600 x 40 mm Plexiglas shear box with vertical confinements of 0.9, 3 and 20 kPa. Observations show that the rubble failure initiates by freeze-bonds breaking. The analyses show that increased freeze-bond strength contributes to higher peak shear stress in the rubble primary failure mode and to the formation of large "block assemblies" when the rubble is breaking. This deformation pattern contributes to an increased dilatation. In the secondary failure mode, the rubble peak shear stress is higher for the tests with the long submersion times, which however present lower freeze bond strength. It is explained by the higher presence of slush between the blocks and the degraded surface of the ice increasing the friction between the blocks.

INTRODUCTION

First year ice ridges are bulky ice features that can pose a major threat to offshore structures. They are composed of numerous ice blocks distributed into the sail and the keel, comprising a consolidated layer at its upper part. Several approaches exist to describe the mechanical behaviour of the rubble ice in the keel. They can be divided into continuum or discrete mathematical models. Continuum models consider the rubble as a continuous material where the particular behaviour of one ice block is not studied but only the global behaviour of the whole

rubble. Therefore deriving the mechanical properties suitable for such type of models requires the study of a volume of rubble which is sufficiently large to avoid that the behaviour of one particular ice block introduces large variations in the global behaviour of the whole rubble, i.e. representative volume element (RVE).

A precise continuum description of this material is prevented by the lack of full scale data, due to the requirement of a too large RVE which implies that physical tests should reach impractical dimensions. Model scale investigations can provide insights into understanding the concepts governing the rubble behaviour, but the scaling of its properties is still a matter of research (Høyland, 2010; Repetto-Llamazares, 2010).

The two main types of tests used for investigations of the rubble ice mechanical behaviour are punch tests and the shear box tests. The first one presents the advantage of having the possibility to study the rubble without extracting it from the keel. But its interpretation requires the use of advanced numerical tools due to unknown boundary conditions and the number of parameters to derive being larger than the number of available equations. On the contrary, a shear box must be filled with rubble ice, but its boundary conditions are well controlled. Early tests used direct shear box (Prodanovic, 1979; Weiss et al., 1981; Hellmann, 1984; Fransson and Sandkvist, 1985). These tests present the advantage of simplicity but the rubble has to fail along a specified failure plane, preventing from getting reliable quantitative results (Timco and Cornett, 1999). Other tests were then performed with a simple shear box (Urroz and Ettema, 1987), bi-axial compression chambers (Sayed, 1987; Timco et al., 1992) and Wong et al. (1990) used a small tri-axial cell.

Freeze-bonding between the ice blocks has been acknowledged as one of the physical mechanisms giving the rubble ice its peculiar aspects in comparison with other geotechnical materials such as sand and gravel. From pseudo-discrete continuum models of direct shear tests, Liferov (2005) and Shafrova (2007) showed that the freeze-bond properties are important for the strength evaluation and deformation behaviour of ice rubble. They are responsible for the cohesive strength of the rubble. However, it can be supposed that most of the freeze bonds are destroyed at the beginning of the deformation process, and Ettema and Urroz (1991) argue that rubble undergoing continuous shear is essentially cohesionless. From these observations, Liferov and Bonnemaire (2005) deduce that rubble ice presents two types of failure mode:

- The primary failure mode is controlled by the initial strength of the rubble skeleton (the freeze-bonds network joining the blocks). The frictional resistance of the rubble is not mobilized.
- The secondary failure mode where substantial deformations have already occurred and the rubble strength is dominated by the frictional resistance.

They used this assumption to suggest a revision to the 3 phases description of the rubble deformation in the shear box tests of Hellmann (1984). In the first phase, up to 2 mm of displacement (the displacement in the entire test is 480 mm), a steep increase of the shear force is observed to up to 60% of the maximum force. Liferov and Bonnemaire (2005) attribute it to the breakage of the rubble skeleton. In the second phase, the peak force is reached and extensive dilatation is observed. Finally in the phase 3, the rubble critical state is reached (no more variation of the shear strength upon further deformation).

In continuous modelling of the rubble behaviour, the freeze-bond failure is represented by a material model including cohesion softening (Heinonen, 2004; Serré, 2011), and in discrete

element modelling, by the breakage of each individual freeze-bond (Polojärvi and Tuhkuri, 2010). Serré (2011) shows the importance of the cohesion softening in the simulation of the post peak load behaviour in punch test analysis. Repetto-Llamazares et al. (2011b) measured the cohesion softening in the shear testing of individual freeze bonds. However no authors have yet related the freeze-bond properties to the shear strength and cohesive properties of the rubble.

The present paper is the first part of a series of two papers that relate qualitatively the freeze-bond properties to the rubble deformation behaviour through shear box and freeze bond testing. It focuses on the 2D shear box testing of the rubble and gives a detailed description of the failure mechanism and how it is affected by the level of freeze-bonding. Part II (Repetto-Llamazares et al., 2011c) gives the testing results of individual freeze-bonds extracted from the rubble, and compares the experimental results with the numerical simulations of Shafrova (2007).

EXPERIMENTAL METHOD

Rubble ice

The experiments were performed in the cold laboratory of the department of Civil and Transport engineering at NTNU. The laboratory is equipped with a tank for growing ice (FRYSIS II). It is 0.8 m x 1.2 m x 1.3 m (depth) with heated walls and bottom. The air temperature in the laboratory was held at -20 °C in order to freeze saline water (8 ppt) in the tank. A 20 cm layer of columnar saline ice was grown.

The rubble ice was composed of ice blocks presenting all the same dimensions. They were cut with a band saw from the ice sheet grown in the tank. The block dimensions were 60 mm x 40 mm x 22 mm. They scale with a ratio 1:20 to the observations of Høyland (2007) in the Barents Sea where full scale average block dimensions of 1.2 m x 0.8 m x 0.44 m are given Once the blocks were produced, they were stored in plastic boxes at -7 °C. The ice at the time of testing had a salinity of 3 ppt.

The strength of the ice blocks was estimated with uniaxial compression tests and three-point bending tests as shown in Figure 1. The supports in these tests were built from wood, which is not stiff enough to give accurate measurements, but good enough for our purpose.

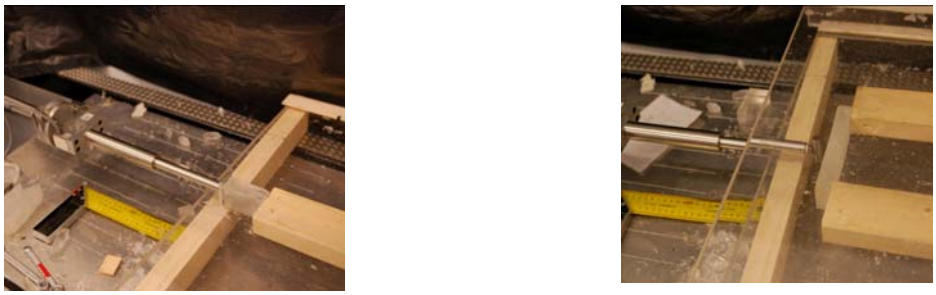

a) b)

Figure 1. Compression test in (a) and 3-points bending test in (b).

The piston speed was equal to the speed used during shear box testing (0.0016 m/s giving a compressive strain rate of 2.6 10^{-2}/s and a flexural strain rate of 1.7 10^{-2}/s. A load cell with a maximum capacity of 5 kN was used for the compression test and 1 kN for the bending test. The sampling rate was 10 Hz. Each block strength test was performed 4 times for each type of rubble.

Two rubble types were produced for the shear box experiment. The first type was composed of colder and less eroded ice blocks since the rubble was submerged only 10 min. The second type was submerged for 20 h, and thus became warmer and more eroded.

Shear Box

A schematic drawing of the shear box is shown in Figure 2. It consisted of three main sections: a lower part that was fixed to a stiff metal frame, an upper part that slid on top of the lower part and a sliding roof supported only by the rubble. Weights placed on this roof applied the normal confinement on the rubble. The upper part was moved by a velocity controlled hydraulic piston. The force exerted by the piston was recorded with a sampling rate of 1 Hz by a load cell with maximum capacity of 5 kN. The velocity during each test was constant, but in between tests it varied from 0.0012 m/s to 0.0020 m/s (average value 0.0016 m/s). The box had holes in the bottom of the lower part to allow water to drain out after submersion.

The upper part was supported by steel wheels rolling on a lubricated rail. The friction of the rolling system in similar conditions to the ones used during testing was measured to be 11 N and this amount was subtracted from all the force time series during the analysis of the results.

The size of the shear box should in principle contain at least one RVE. For continuum (non-localized) behaviour it is often given as 10 times the size of the heterogeneities (Lemaitre and Chaboche, 1990). However there is no agreement yet on the size of the RVE for rubble ice. Therefore the shear box length (600 mm) was tentatively selected to be 10 times larger than the block length. Its width (40 mm) was equal to the width of the ice blocks in order to study the behaviour of the rubble in two dimensions only and remove the complications linked to 3D effects. The shear box dimensions are given in the drawing of the shear box during testing (Figure 3). A 100 mm high wooden board was placed in the bottom of the shear box.

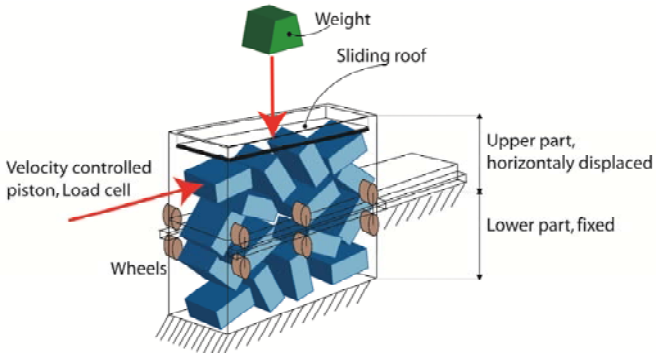

Figure 2. Schematic representation of the set up used in the rubble shear experiments.

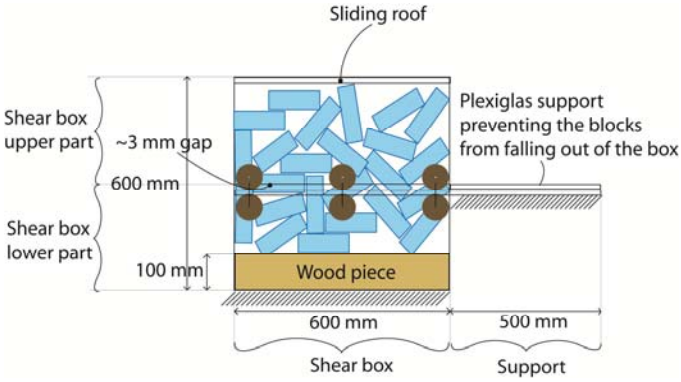

Figure 3. Drawing and dimensions of the shear box.

Experimental Procedure

The shear box was filled by placing each individual ice block manually in random positions inside the box until the rubble height (h_r) was approximately 400 mm. The number of blocks (N_b) in each test was recorded and the initial porosity (η) computed as:

$$\eta = 1 - \frac{N_b h_b L_b}{h_r L_B} \tag{1}$$

where h_b represents the block thickness, L_b the block length and L_B the shear box length. The porosity varied between 20 to 40 % with an average value plus/minus one standard deviation of 32 ± 5 % (Table 1).

Once the filling was completed, the shear box was submerged into a secondary basin of dimensions 0.8 m x 1.2 m x 0.6 m (Figure 4) that contained saline water with a salinity equal to the salinity from the ice tank (8 ppt). The air temperature of the secondary tank's room was set to -1°C and the water was at its freezing point (-0.3 °C). During submersion, the normal confinement over the rubble was the same in all the tests and equal to 655 Pa (weight of the sliding roof). The experiments were performed using two different submersion times (Δt): 20 hours, referred as *long* tests, and 10 minutes, referred as *short* tests. After submersion, the shear box was removed from the water, left for a couple of minutes to drain, and placed in the stiff metal frame for mechanical testing (Figure 5).

Figure 4. Shear box filled with the rubble and submerged into the secondary basin.

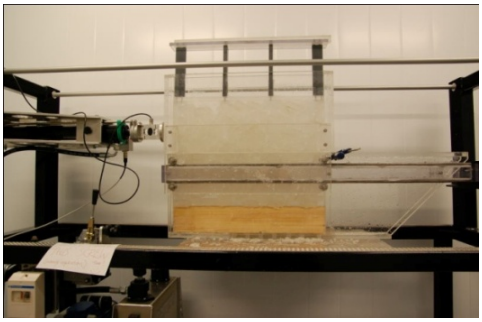

Figure 5. Shear box placed into the stiff metal frame ready for the mechanical testing.

The air temperature during the mechanical tests was set to -7°C. During the shear test two different normal confinements (σ) were used: 3020 Pa, referred as *High* tests, and 860 Pa,

referred as *Low* tests. The confinement values were selected from Ettema and Schaeffer (1986). The highest one corresponds to the vertical stress caused by buoyancy that can be expected in a 10-m deep keel. The rubble peak shear stress was measured three times for each combination of the two different submersion times and the two normal confinements. Two extra experiments were performed to test extreme conditions: test Extra_High_Short was performed by using the weight of one of the authors as normal confinement (estimated to be 50 kg) while test Dry_Low was done using ice that had not been submerged. Table 1 shows the main parameters from each test.

Table 1. Test matrix of the shear box experiments specifying the normal confinement σ, the submersion time Δt, the rubble height h_r, the number of blocks N_b and the porosity η.

σ [Pa]	Δt [hr]	h_r [m]	N_b	η [%]	Test Name
3020 (High)	20 (Long)	0.450	132	35.5	High_Long_1
		0.471	123	42.6	High_Long_2
		0.364	131	20.8	High_Long_3
	0.17 (Short)	0.405	123	33.2	High_Short_2
		0.425	131	32.1	High_Short_4
		0.425	126	34.7	High_Short_5
860 (Low)	20 (Long)	0.491	158	29.3	Low_Long_1
		0.456	142	31.5	Low_Long_2
		0.386	132	24.8	Low_Long_3
	0.17 (Short)	0.406	127	31.2	Low_Short_1
		0.439	133	33.3	Low_Short_2
		0.399	129	28.9	Low_Short_3
	0	0.446	127	37.4	Dry_Low*
20500	0.17	0.446	127	37.4	Extra_High_Short

* The ice has not been previously submerged

RESULTS

Force-time diagrams

Figure 6 shows six representative curves of force vs. time for different submersion times (Short, Long and Dry). The two lower confinements did not seem to produce any significant difference. We could identify three phases as described by Hellmann (1984).

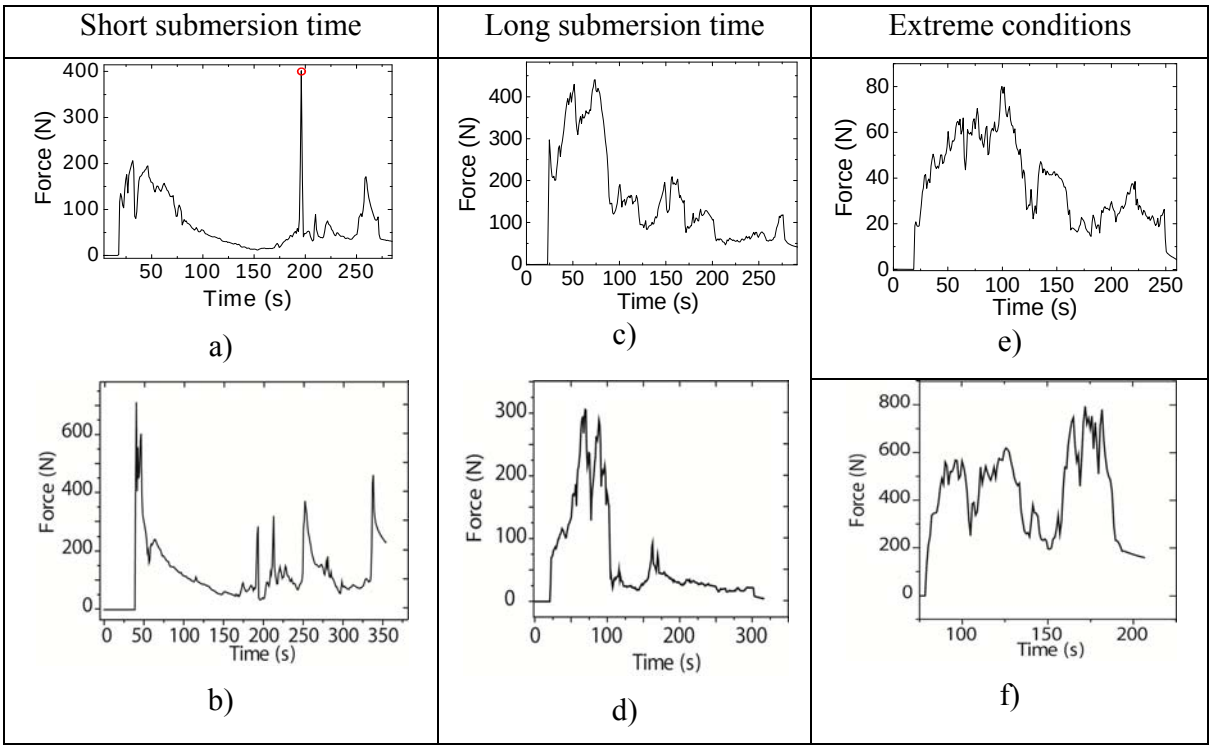

Figure 6. Representative force time series from the shear box test. a) High_Short_5; b) Low_Short_1; c) High_Long_1; d) High_Long_2; e) Dry_Low; f) Extra_High_Short. The peak load in the red circle in (a) corresponds to the breaking of the ice block in Figure 11 b).

Phase 1:

The force increased quickly during the first few seconds, and we chose to define Phase 1 as the first 6 seconds after the load started to increase in order to be sure it was long enough to include the initial sharp force increase of each test. The average rubble peak shear stress in phase 1 is given in Figure 7.

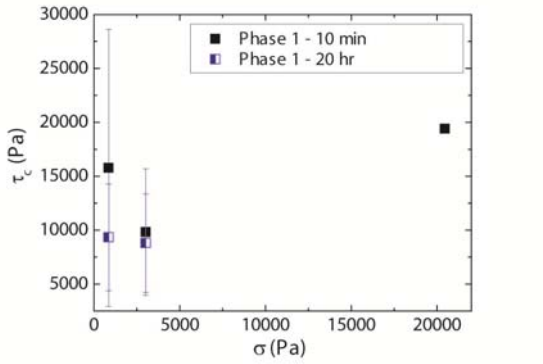

Figure 7. Rubble peak shear stress in phase 1.

Phase 2:

As a general trend the following described phase 2. After the initial sharp increase the load continued to increase but at a slower rate, with numerous peaks randomly mounted on the base line. The load reached maximum value and then decreases. For analyses purposes, this phase was defined as extending from 6 to 120 s, whereas it ends when the peak load is reached in Hellmann (1984). The 120 s threshold was selected such that the peak stress was included in phase 2. After 120 s the load presented a general decreasing trend in all the tests. The difference between the maximum load and the load at the end of the initial fast load increase is more pronounced for the

tests with long submersion times (Figure 6b) than for those with short submersion times (Figure 6a). The difference is even larger in the test where the rubble was tested dry (Figure 6c).

Phase 3:

The load decreases and tends to stabilize, although random peaks are also observed in this phase. Phase 3 lasts from 120 s to the end of the test, selected as 230 s, the time at the end of the shortest test.

It should be noted that not all the tests agree to the previous description. Figure 8 shows the load curve of the test Low_Long_3. The rubble extrusion occurred later than in the other tests and ice blocks were trapped between the upper left and lower right side of the box at the end of the test. Therefore the load curve increased toward the end of the test on contrary to what was usually observed. The load increase toward the end of the test reflected more an effect from the boundary conditions than from the material behaviour. Low_Long_3 was an exception also among the Low_Long tests, whose behaviour generally followed the previous description.

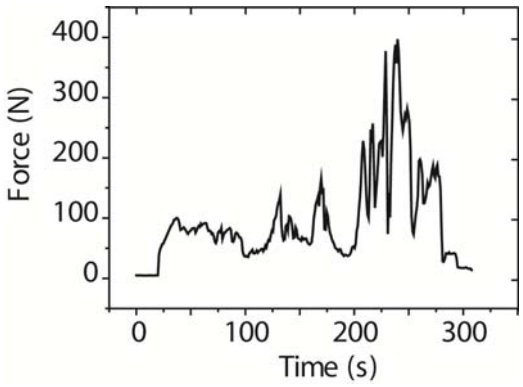

Figure 8. Load time series for test Low_Long_3

Deformation mechanisms

The failure mechanism always started by a crack formation linked to freeze bond failure. The rubble was partitioned in several portions consisting of ice blocks freeze-bonded together (phase 1). These portions are here referred as "block assemblies". Then the cracks grew and later the blocks freshly separated collapsed. Afterward, block and block assemblies rotation, rearrangement, and formation of new cracks within the block assemblies were usually observed (phase 2 and 3). It was challenging to determine visually the transition between the phases. The pictures in Figure 9 show a characteristic crack growth during the test High_Long_1. During the deformation, the confinement inside the rubble was pressing some blocks against each other, thus creating "force chains" in the material: several blocks in contact with each other form a line and compressive forces can thus be transmitted between the two extremities of the line. During the tests the rubble was extruded vertically by sliding against the side of the shear box in contact with the piston (Figure 10). Some of the tests also revealed that individual ice blocks or small block assemblies were rotating at the interface between the two parts of the shear box (shear interface).

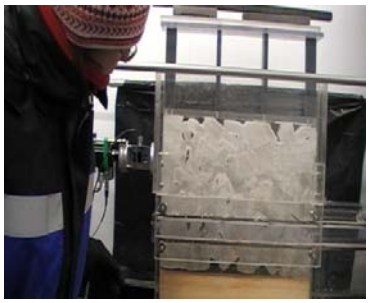

a)

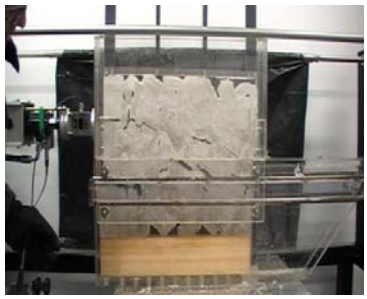

b)

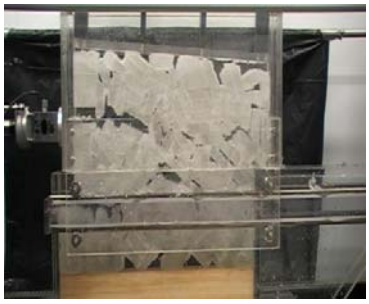

c)

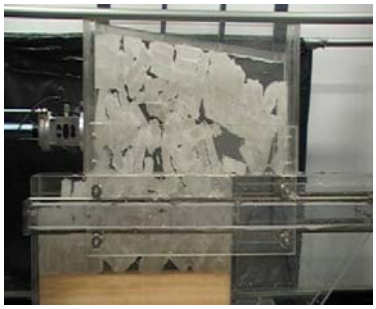

d)

Figure 9. Pictures of the test High_Long_1 showing characteristic crack growth during testing. a) initial state, 0 s; b) crack initiation, phase 1, 34 s; c) crack growth, phase 2, 50 s; d) rubble collapse and rearrangement, 123 s. The time is given from the beginning of the time series in Figure 6 c).

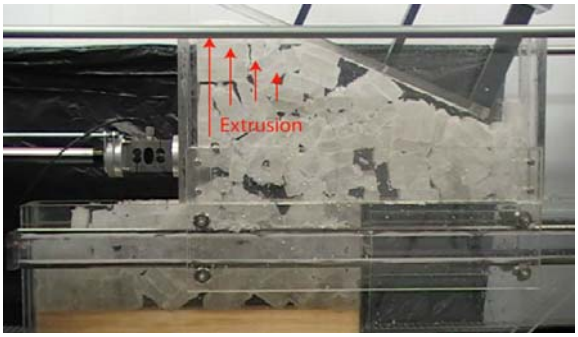

Figure 10. Pictures of the test High_Long_1 showing rubble extrusion, phase 3, 194 s.

Block failure

Visual inspection of the surface of the rubble lying in the lower part of the shear box after testing revealed that in 10 of the 12 tests, ice blocks were broken at the shear interface (Figure 11a). Unfortunately it was only possible to determine visually when the blocks broke in two tests. In the test High_Short_2 one block broke in bending mode. The breaking occurred while the measured force was decreasing but no particular point of the time series could be associated to the event. In the test High_Short_5 one block was trapped between several ice blocks and the lower edge of the pushing side. The block was compressed along its longest side and failed in splitting mode (Figure 11b). The failure was accompanied by a sound and a peak was recorded in the force-time signal (Figure 6a).

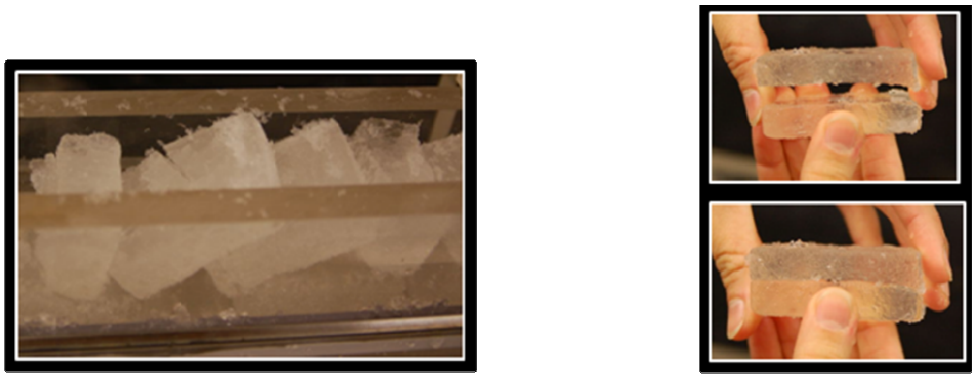

a) b)

Figure 11. a) broken blocks at the box shearing interface in test High_Short_2; b) block broken in splitting in test High_Short_5.

The uniaxial compression strength (σ_c) and flexural strength (σ_f) of the ice blocks submerged in water during 10 min and 20 hours are given in Table 2 together with the Mohr-Coulomb cohesion c and friction φ, assuming the ice mechanical behaviour can be described by the Mohr-Coulomb model.

Table 2. Ice block properties for short and long submersion times. Both measured (flexural and uniaxial compressive strength and salinity) and derived (cohesion c and friction angle φ).

Δt [hr]	σ_f [MPa]	σ_c [MPa]	S [ppt]	c [MPa]	φ [°]
0,17	0.42 ± 0,1	3,0 ± 0,7	3	0.56	50
20	0,13 ± 0,04	2,4 ± 0,7	3	0.27	64

Dilatancy

The dilatancy characterizes the volume increase of the rubble during shearing. The tests with short submersion times showed higher dilatancies than the ones with long submersion times. A typical difference in the dilatancy of short and long tests is given in Figure 12 where the rubble volume and porosity increased more for the short submersion time tests than for the long ones.

The range of normal confinements between 500 and 3000 Pa did not affect the dilatancy. However, an important reduction of the dilatancy was observed in the Extra_High confinement test (Figure 12c), where only little volume change of the rubble could be observed during testing. The number of broken blocks was not different in this test than in the other ones.

a) b) c)

Figure 12. Dilatancy effects after 30 s of deformation (phase 2). a) short submersion time with a high dilatancy; b) long submersion time tests with lower dilatancy; c) extra high confinement test where the rubble volume did not increase.

Rubble shear deformation energy

The deformation energy for each phase (U_d) is defined as the amount of energy transferred from the piston to the shear box. It is computed for the three phases of each test according to Equation 2:

$$U_d = v\int_{t_S}^{t_F} F_T(t)dt \qquad (2)$$

where v represents the piston's velocity (1.6 10^{-3} m/s), t_s and t_F the time at the beginning and end of each phase, and F_T the force exerted by the piston. It is then divided by the phase time length Δt_{ph} and the number of blocks N_b to obtain the deformation power per block P_b as shown in Equation 3:

$$P_b = \frac{U_d}{N_b \Delta t_{ph}} \qquad (3)$$

The values of P_b obtained for each phase and submersion time are plotted against the normal confinement in Figure 13a) and a schematic drawing of P_b evolution during shearing is given in Figure 12b). For the short submersion time tests, Figure 13 shows that the power was the highest in phase 1. It then decreased in phase 2 and became minimal in phase 3. For the long submersion time however, phase 2 presented the highest power, then closely followed by phase 1 and finally phase 3. P_b for the Extra_High_Short test is not given in Figure 13. It was equal to 0.0004 W in phase 1 and 0.0073 W in phase 2. These two values are respectively the lowest of all the phase 1 P_b values and the highest of all the phase 2 P_b values.

When comparing between short and long submersion time tests, only the power in phase 1 is higher in the short submersion time tests. Phase 2 and phase 3 present a higher power than phase 1 in the long submersion time tests.

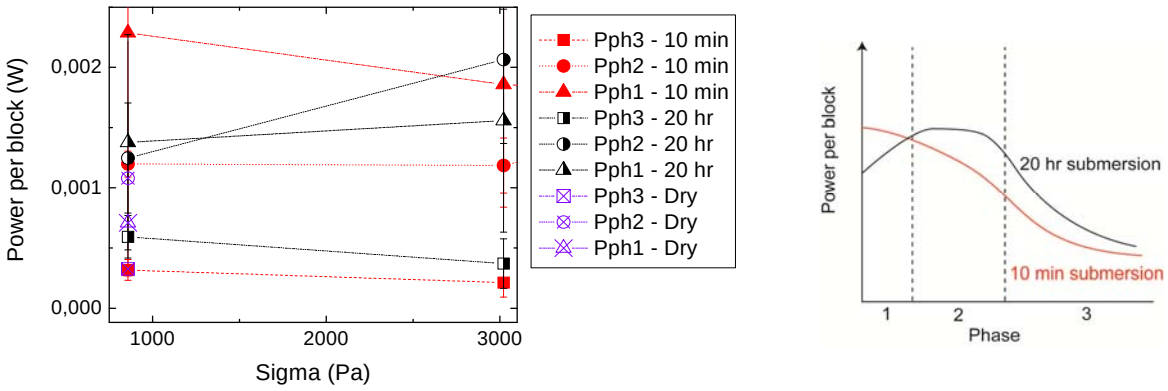

a) b)

Figure 13. P_b as a function of the confinement, for each phase and submersion time (a) and representation of P_b evolution during deformation.

The power required to deform the rubble in the shear box is plotted for all the phases and all the submerged tests with the exception of the tests Extra_High_Short test as a function of the porosity in Figure 14. A slight tendency to lower power for higher porosities appears, but the highest powers can be found in the middle of the porosity range, which makes the result interpretation of the results difficult. However the test with the highest porosity showed the lowest deformation power.

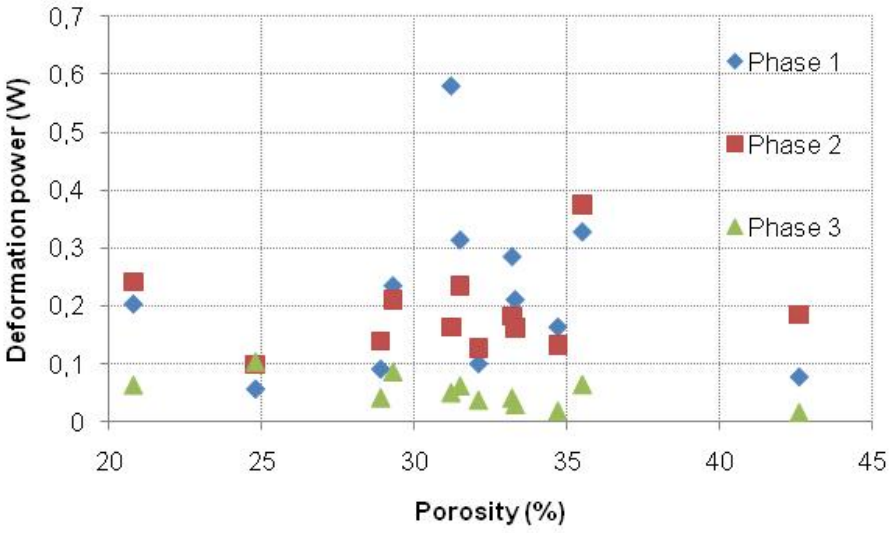

Figure 14. Deformation power of the rubble as a function of the initial porosity.

DISCUSSION

Dilatancy

The dilatancy characterizes the volume increase of the rubble during shearing. In pressure dependent material models used for instance in Liferov et al. (2003), Heinonen (2004) or Serré (2011) it is represented by the dilatancy angle which determines the shape of the plastic flow potential. Very limited information is available on the dilatancy angle of rubble ice but Liferov et al. (2003) showed by performing finite element analysis of punch tests that an increase of rubble dilatancy produced a higher resistance to the punch test action. The effect of the submersion time and thus the freeze-bond strength on this parameter is investigated qualitatively, but not quantitatively.

A comparison between the test with dry rubble ice and the other tests revealed that freeze-bonding played an important role in the dilatant behaviour of the rubble. In the dry test the rubble was not submerged before testing and therefore the freeze-bonding between blocks was either very low or nonexistent (Ettema and Schaefer, 1986; Repetto-Llamazares et al., 2011a). The rubble dilatancy during this test was much lower than during the tests on submerged rubble. The videos revealed that after submersion the freeze-bonding prevented the blocks from sliding relatively to each other. Consequently large block assemblies were displaced into the rubble during shearing thus increasing the rubble volume. Figure 15 gives an example of a block assembly formed by freeze-bonding. The freeze bond effect on the dilatancy is also visible in the comparison between the tests with short and long submersion time (Figure 12 a and b). The short tests showed a higher dilatancy than the long ones. This observation is in good agreement with the measurements of higher freeze-bond strengths for short submersion times (Repetto-Llamazares et al., 2011c).

The increase in the size of the block assemblies with freeze bonding indicates that the RVE should be sensitive to the degree of freeze bonding. As a matter of fact, the RVE should contain a sufficient amount of block assemblies such that the unique behaviour of one particular block assembly does not affect the global behaviour of the RVE. In the tests with the two lower levels of confinement, some of the “force chains” extended all across the rubble. It might indicate that at least in this test configuration, the shear box size was below the RVE size.

In the Extra_High_Short test we could not observe any significant volumetric expansion which means the dilatancy decreased with increasing confinement stress. It is reasonable to estimate that the freeze-bonds are not strong enough to maintain the integrity of the block assemblies submitted to high stress levels. The reduced size of the assemblies then reduces the dilatancy.

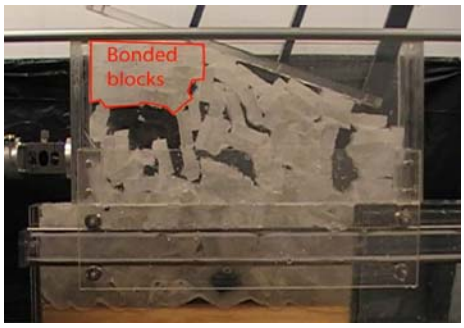

Figure 15. Freeze-bonding causes the displacement of large block assemblies (phase 2).

It should be noted that the in-situ dilatancy of first year ice rubble is expected to be lower than the one observed in the 2D experiments since in a 3D configuration the ice blocks can rotate with more degrees of freedom allowing more compaction in the rubble. However the qualitative dependence of the dilatancy with the submersion time, normal confinement and freeze-bonding that is observed in the present experiment should be the same for 3D conditions. The breakage of the rubble into several assemblies of freeze-bonded blocks is also observed after ridge-interaction with structures at different scales. Figure 16a) shows a block assembly which drifted out of the keel after the interaction between a structure and a 0.5-m deep keel of a model ice ridge (Serré et al., 2009). Figure 16b) shows a corresponding situation in-situ in the Fram Strait, after R/V Lance had impacted an ice ridge in September 2009. The freeze-bonding between the blocks is clearly visible in the picture given in Figure 16c), taken after the breakage of a ridge in the Barents Sea in May 2009.

a)

b)

Picture from Vegard Aksnes

c)

Figure 16. Freeze-bonded block assemblies after ridge impact are also observed in model tests of ridge structure interaction described in Serré et al. (2009) (a) and in-situ after interaction with R/V Lance in the Fram Strait (b) and in the Barents Sea (c).

Rubble shear deformation energy

The power plots show that different mechanisms dissipate the deformation energy during the rubble shearing.

- The deformation power in phase 1 is correlated to the amount of freeze-bonding since P_b is:

  - the highest for the tests with short submersion time and the part II of the present paper reveals that these tests presented the strongest freeze-bonds.

  - the lowest when no freeze bonds are present (Dry_Low test).

  This observation is in agreement with the hypothesis of Liferov and Bonnemaire (2005) about the breaking of the rubble skeleton as being the main contributor to the ridge action in the initial stage of a ridge/structure interaction.

- Friction and interlocking are the main contributors to the rubble resistance in phase 2 and 3. The rubble skeleton being broken in phase 1, the rubble deformations can localize in the crack zones. The remaining freeze-bonds contribute to a less extent to the rubble resistance in phase 2 and 3, which is now dominated by friction and interlocking between the ice blocks. The effect of the ice-ice friction on the rubble resistance is shown by P_b in phase 2 and 3 being higher for the long submersion time tests. The ice-ice friction was supposed to be higher in these tests due to the warmer ice and higher amount of slush that grew in between the blocks (Figure 17). Keinonen and Nyman (1978) indicated that submersion deteriorates the surface of ice blocks and increase their roughness and friction coefficient. The hypothesis of slush increasing the rubble friction angle is mentioned in Liferov and Bonnemaire (2005). The ice-ice friction dependence on the surface state of the ice and the amount of slush is confirmed by the low P_b values in the dry tests where the ice was the coldest and cleanest (smooth surface and no slush).

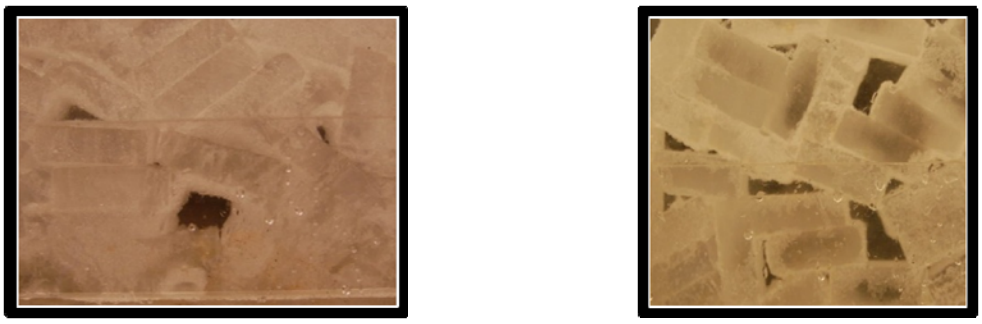

a) b)

Figure 17. A larger amount of slush has grown between the ice blocks in the long submersion time tests in (a) while the blocks are still distinct from each other in the short submersion time tests (b).

The lower P_b in phase 2 and 3 for the short submersion time tests (compared with the long submersion times) can also be caused by the initial higher freeze-bonding causing a stronger localization of the deformation. Actually the destruction of the freeze-bonds contributes to the rubble softening which is a phenomenon usually associated with a localized growth of the deformation (Belytschko et al., 2000). A localized failure zone then decreases the amount of ice blocks sliding on each other and thus the deformation energy of the rubble becomes lower.

When considering short and long submersion time tests, the short submersion time tests present the highest phase 1 P_b value but the lowest phase 2 P_b value. It might reveal that in young ice

ridges the freeze-bonding would the main contributor to the rubble action, while in old first year ice ridges it would be the friction between the ice blocks.

The low values of P_b in phase 3 might also be explained by the consequent portion of the shear box upper part sliding over the Plexiglas plate. The ice-ice friction at the shear interface is then progressively replaced by an ice-Plexiglas friction, which could influence the value of P_b. Unfortunately this friction coefficient was not measured. It is estimated to 0.02 for HSVA model ice (Serré et al., 2009). The ice-ice friction is given in Repetto et al. (2011c).

The Extra_High_Short test is a particular case since it was submitted to a confinement 7 times higher than any of the other tests. It presents the lowest of all the phase 1 P_b values and the highest of all the phase 2 P_b values.

- The low P_b in phase 1 might be explained by the freeze-bonds which could have been broken while the confinement was applied, just before shearing. The ice blocks could then accommodate small displacements without opposing a so large resistance as if they would have been frozen together.
- The high P_b in phase 2 might be explained by the energy required by the rubble dilation to lift-up the confinement weight. No significant dilatation could be observed in comparison to the other tests, but it is possible to assume that accurate measurements would have monitored a small uplift of the rubble surface.

The friction angle should be measured when the rubble reaches its critical state (the shear strength becomes independent of the strain). Phase 3 is therefore the most suitable phase for the estimation of the effect from the frictional resistance. However the rubble was sliding partly over the Plexiglas and in all the tests with an initial confinement of 0.9 and 3 kPa, the rubble extrusion caused the weights to fall from the shear box roof at the beginning of this phase. Consequently all the tests present the same confinement in phase 3 apart from the Extra_High_Short test. Therefore numerous assumptions are necessary for the computation of the friction angle, which is then left outside the scope of this paper.

CONCLUSION

14 shear box tests with laboratory made ice rubble were performed in order to relate the freeze bond strength to the peak shear stress and failure behaviour of rubble ice. The rubble ice was submerged for different time length before testing and Part II gives a link between the submersion time and the freeze-bond strength. The present paper shows that a primary and a secondary failure mode could be observed and that the rubble failure was initiated by freeze-bond failures. With respect to the freeze-bonds it was observed that:

- The freeze-bonds are important for the ice rubble behaviour as stronger freeze-bonds gave higher deformation power in Phase 1, higher strain localization, larger block assemblies and higher dilatation (volumetric expansion)
- The importance of the freeze-bonds for the rubble behaviour becomes less the more eroded the rubble is and the higher the confinement (hydrostatic stresses)

In rubble ice where the ice blocks and freeze bonds have been eroded by the water during long submersion times, the frictional resistance between the ice blocks is the main contributor to the rubble action.

AKNOWLEDGMENTS

The authors would like to express their gratitude to Dr. Pavel Liferov for his comments. The discussions with Prof. Ibrahim Konuk on the conception of the shear box test were also appreciated, and of course the help from Gustav and M-Tech for its realisation. These tests could not have been realised without the support of Prof. Sveinung Løset and the financial contribution from the PetroArctic and the PetroRisk projects, part of the Petromaks project of the Research Council of Norway with additional sponsoring from Statoil and DNV.

REFERENCES

Belytschko, T., Liu, W. K. and Moran, B., 2000. Nonlinear Finite Elements for Continua and Structures. John Wiley & Sons, Ltd., Chichester, England.

Ettema, R. and Schaefer, J.A., 1986. Experiments on freeze-bonding between ice blocks in floating ice rubble. Journal of Glaciology 32 No 112, pp. 397–403.

Ettema R. and Urroz G.E., 1991. Friction and Cohesion in Ice Rubble Reviewed. Proceedings of the 6th International Speciality Conference Cold Regions Engineering, Hanover, USA, pp. 316-325.

Fransson, L. and Sandkvist, J., 1985. Brash ice properties—laboratory tests, Proc. of the 8th Int. Conf. on Port and Ocean Engineering under Arctic Conditions Narssarssuaq, Greenland vol. 1, pp. 75–87.

Heinonen, J., 2004. Constitutive modelling of ice rubble in first-year ridge keels. PhD thesis, Helsinki University of Technology.

Hellmann, H., 1984. Basic investigations of Mush Ice, Proc. of the 7th Int. Symp. on Ice. Hamburg, Germany vol. 3, pp. 37–55.

Høyland, K. V., 2007. Morphology and small scale strength of ridges in the North-western Barents Sea. Cold Regions Science and Technology, vol 48, issue 3, pp 169-187.

Høyland, K. V., 2010. Thermal aspects of model basin ridges. Proc. of the 20th Int. Symp. on Ice. Lahti, Finland, Paper No. # 66.

Keinonen, A. and Nyman, T., 1978. An experimental model-scale study on compressible, frictional and cohesive behaviour of broken ice masses, Proc. of the Int. Symp. on Ice. Lulea, Sweden vol. 2, pp. 335–353.

Lemaitre, J. and Chaboche, J.-L., 1990. Mechanics of Solid Materials. Cambridge University Press, Cambridge, UK.

Liferov, P., Jensen, A. and Høyland, K., 2003. 3D finite element analysis of laboratory punch tests on ice rubble. Proceedings of the 17th International Conference on Port and Ocean Engineering under Arctic Conditions, POAC, Trondheim, Norway, vol. 2, pp. 611–621.

Liferov, P., 2005. Ice rubble behaviour and strength: Part II. Modelling. Cold Regions Science and Technology, vol. 41, issue 2, pp 153-163.

Liferov, P. and Bonnemaire, B., 2005. Ice rubble behaviour and strength: Part I. Review of testing and interpretation of results. Cold Regions Science and Technology, vol 41, issue 2, pp 135-151.

Polojärvi, A. and Tuhkuri, J., 2010. Discrete Element Simulation of Ridge Keels with Freeze Bonds. Proc. of the 20th Int. Symp. on Ice. Lahti, Finland.

Prodanovic, A., 1979. Model Tests of Ice Rubble Strength. Proceedings of the 5th International Conference on Port and Ocean Engineering under Arctic Conditions, POAC, pp.89-105.

Repetto-Llamazares, A. H. V., 2010. Review on model ice ridges, Proceedings of the 20th IAHR International Symposium on ice, June 14-17, Lahti, Finland, Paper No. # 154.

Repetto-Llamazares A. H. V., Høyland K. V. and Evers K-U. 2011a. Experimental studies on shear failure of freeze-bonds in saline ice part I: Set-up, Failure Mode and Freeze-bond Strength. Journal of Cold Regions Science and Technology, doi:10.1016/j.coldregions.2010.12.001.

Repetto-Llamazares A. H. V., Høyland K. V. and Kim, E. 2011b. Experimental studies on shear failure of freeze-bonds in saline ice part II: Ice-ice friction after failure and failure energy. To be Cold Regions Science and Technology, doi:10.1016/j.coldregions.2010.12.002.

Repetto-Llamazares, A. H. V. and Høyland, K.V. (2011). Experiments on freeze-bonds and rubble strength Part II: freeze-bonds and comparison with literature. Submittted to POAC 2011, Montreal, Canada.

Sayed, M., 1987. Mechanical properties of model ice rubble. Proc. Struct. Cong. '87, ASCE, New York, USA, pp. 647–659.

Serré, N., 2011. Mechanical properties of model ice ridge keels. Submitted to Cold Regions Science and Technology.

Serré N., Liferov, P., Jochmann, P., 2009b. Model testing of ridge keel loads on structures Part III: investigation of model ice rubble mechanical properties. Proceedings of the 20th International Conference on Port and Ocean Engineering under Arctic Conditions, POAC, Luleå, Sweden.

Shafrova, S., 2007. Initial failure of the ice rubble in plane strain direct shear tests. Proceedings of the 19th International Conference on Port and Ocean Engineering under Arctic conditions, POAC, Dalian, China, vol. 1, pp. 256-266.

Timco, G.W., Funke, E.R., Sayed, M. and Laurich, P.H., 1992. A laboratory apparatus to measure the behaviour of ice rubble. Proc. of Offshore Mechanics and Arctic Engineering Conf. Calgary, Canada vol. IV, pp. 369–375.

Timco, G.W., and Cornett, A.M., 1999. Is φ a constant for broken ice rubble? Proc. of the 10th Workshop on River Ice Management with a Changing Climate. Winnipeg, Manitoba, Canada, pp. 318–331.

Urroz, G.E. and Ettema, R., 1987. Simple shear box experiments with floating ice rubble, Cold Regions Science and Technology 14, pp. 185–199.

Weiss, R.T., Prodanovic, A. and Wood, K.N., 1981. Determination of ice rubble shear properties, Proc. of the Int. Symp. on Ice. Quebec, Canada vol. 2, pp. 860–872.

Wong, T.T., Morgenstern, N.R. and Sego, D.C., 1990. A constitutive model for broken ice. Cold Regions Science and Technology 17, pp. 241–252.